SPE 63065

Surrogate Modeling–Based Optimization for the Integration of Static and Dynamic Data Into a Reservoir Description

Nestor V. Queipo, SPE, Salvador Pintos, Néstor Rincón, Nemrod Contreras, and Juan Colmenares, Applied Computing Institute, Faculty of Engineering, University of Zulia, Venezuela

This paper was prepared for presentation at the 2000 SPE Annual Technical Conference and Exhibition held in Dallas, Texas, 1–4 October 2000.

Abstract

This paper presents a solution methodology for the problem of estimating the distributions of permeability and porosity in heterogeneous and multiphase petroleum reservoirs by matching the static and dynamic data available.

The solution methodology includes, the construction of a "fast surrogate" of an objective function whose evaluation involves the execution of a time-consuming mathematical model (i.e. reservoir numerical simulator) based on neural networks, DACE modeling, and adaptive sampling. Using adaptive sampling, promising areas are searched considering the information provided by the surrogate model and the expected value of the errors.

The proposed methodology provides a global optimization method, hence avoiding the potential problem of convergence to a local minimum in the objective function exhibited by the commonly Gauss-Newton methods. Furthermore, it exhibits an affordable computational cost, is amenable to parallel processing, and is expected to outperform other general purpose global optimization methods such as, simulated annealing, and genetic algorithms.

The methodology is evaluated using two case studies of increasing complexity (from 6 to 23 independent parameters). From the results, it is concluded that the methodology can be used effectively and efficiently for reservoir characterization purposes. In addition, the optimization approach holds promise to be useful in the optimization of objective functions involving the execution of computationally expensive reservoir numerical simulators, such as those found, not only in reservoir characterization, but also in other areas of petroleum engineering (e.g. EOR optimization).

Introduction

The identification of the permeability and porosity parameters that best match the data (static and dynamic) available for a given reservoir is critical for devising an optimal strategy for the development of oil and gas fields. The static data makes reference to those originated from geology, electrical logs, core analysis, fluid properties, seismic and geostatistics; while the dynamic data is represented by field measurements such as, production history, bottom hole pressures from permanent gauges, water-cut, and gas-oil ratio.

Estimating permeability and porosity parameters from available data is difficult because of the following reasons: i) in general, the number of parameters to be estimated are very high, since data is scarce, and the reservoirs are heterogeneous (permeability and porosity have spatial variability), ii) the available data may have very different scope and nature, and, iii) the numerical simulation of the reservoir, necessary to assess how well given permeability and porosity parameters match the available data are computationally expensive.

This paper presents a solution methodology, called NEGO (neural network based efficient global optimization), for the problem of estimating the distributions of permeability and porosity in heterogeneous and multiphase petroleum reservoirs by matching the static and dynamic data available. The solution methodology includes the construction of a "fast surrogate" of an objective function whose evaluation involves the execution of a time-consuming mathematical model (i.e. reservoir numerical simulator) based on neural networks, DACE[1] modeling, and adaptive sampling. Using adaptive sampling, promising areas are searched considering the information provided by the surrogate model and the expected value of the errors.

The DACE surrogate model is initially constructed using sample data generated from the execution of mathematical models with parameters given by a latin hypercube experimental design, and a neural network, and provides error estimates at any point. Additional points are obtained balancing the exploitation of the information provided by the surrogate model (where the surface is minimized) with the need to improve the surface (where error estimates are high). The proposed methodology provides a global optimization method, hence avoiding the potential problem of convergence to a local minimum in the objective function exhibited by the commonly used Gauss-Newton methods[2,3], and computational cost involved in numerically estimating derivatives, and in the step by step movement along given trajectories. Furthermore, it exhibits an affordable computational cost, is amenable to parallel processing, and is expected to outperform other general purpose global optimization methods such as, simulated annealing, and genetic algorithms[4,5].

Problem definition

The problem under consideration is an optimization problem (inverse parameter estimation) with typically a high number of parameters and computationally expensive objective function evaluations. Formally, it can be written as:

$$\textit{find } x \in X \subseteq R^p$$

such that

$f(\mathrm{x})$ is minimized

where f is an objective function of x, the permeability and porosity parameter vector, and X is the set constraint.

The objective function is a measure of the discrepancy between the data (static and dynamic) available and the response of the mathematical models using the current set of parameters. Eq. 1 shows a commonly used form of the objective function (weighted least square version):

$$f(x) = (d_{obs} - d_{calc})' W \left(d_{obs} - d_{calc}\right) \text{.............................(1)}$$

where, W is a weighting matrix, d_{obs} makes reference to static and dynamic data available (normalized), and d_{cal} denotes the corresponding data obtained using a mathematical model.

Hence, the problem of interest is one of finding the vector of parameters x that minimizes the difference between the available data (d_{obs}), and the values calculated (d_{cal}) substituting x in the appropriate mathematical model. Note that a reservoir numerical simulator is necessary for calculating the response associated with dynamic data (e.g. production history). As mentioned before, the reservoir numerical simulator, in general, is computationally expensive and the number of elements in x is usually high, since the data is scarce and the reservoirs are heterogeneous. These two issues place restrictions on the solution approach, given that the number of objective function evaluations are limited to a relatively low value considering the time restrictions typically present in the oil industry.

Solution methodology

The proposed solution approach called NEGO, neural-network based efficient global optimization, is an improved version of the EGO algorithm[6] for the optimization of computationally expensive black-box functions.

The proposed solution methodology involves the following four steps:

1. Construct a sample of the parameter space using the latin hypercube method. The latin hypercube sampling procedure has been shown to be very effective for selecting input variables for the analysis of the output of a computer code[7].
2. Conduct mathematical simulations using the sample from the previous step and record the response values associated with static and dynamic data available, and the objective function values.
3. Construct a parsimonious neural network using the data from the previous step. The purpose of this neural network is to capture the general trends observed in the data; no rigorous performance criteria is placed on the neural network. The input variables of the neural network are the permeability and porosity parameters and the output variable is the corresponding objective function value.
4. Construct a DACE model for the residuals, that is, the difference between the observed objective function values, and the neural network responses using the sample data. These models provide not only estimates of the residuals values but also of the respective errors. The surrogate model for the evaluation of the objective function is the sum of the neural network and DACE models. Details of this step will be given later in this section.
5. Additional points are obtained balancing the exploitation of the information provided by the surrogate model (where the surface is minimized) with the need to improve the surface (where error estimates are high), until a stopping criteria has been met. This balance is achieved by sampling where a figure of merit is maximized. Details of the figure of merit will be given later in this section.

DACE models. These models owe their name, design and analysis of computer experiments, to the title of an article that popularized the approach[1]. These models suggest to estimate deterministic functions as shown in Eq. 2.

$$y(x_j) = \mu + \varepsilon(x_j) \text{..(2)}$$

where, y is the function to be modeled, μ is the mean of the population, and ε is the error with zero expected value, and with a correlation structure given by Eq. 3.

$$\mathrm{cov}(\varepsilon(x_i), \varepsilon(x_j)) = \sigma^2 \exp\left(-\sum_{h=1}^{p} \theta_h \left(x_i^h - x_j^h\right)^2\right) \text{.....................(3)}$$

where, p denotes the number of dimensions in the vector x, σ, identifies the standard deviation of the population, and, θ_h is a correlation parameter, which is a measure of the degree of correlation among the data along the h direction.

Specifically, given a set of n input/output pairs (x, f), the parameters, μ, σ, and θ are estimated such that the likelihood function is maximized[1]. Having estimated these values, the function estimate for new points is given by Eq. 4.

$$\bar{y}(x) = \bar{\mu} + r' R^{-1}(y - 1\bar{\mu}) \quad (4)$$

where, the line above the letters denote *estimates*, r' identifies the correlation vector between the new point and the points used to construct the model, R is the correlation matrix among the n sample points, and 1 denotes an n-vector of ones.

The mean square error of the estimate is given by Eq. 5.

$$s^2\left(x^*\right) = \sigma^2\left[1 - r' R^{-1} r + \frac{\left(1 - 1' R^{-1} r\right)}{1' R^{-1} 1}\right] \quad (5)$$

The model is validated through a cross validation procedure, that essentially makes sure that the estimates using all but the point being tested and the actual response values are within an specified number of standard deviations. The original EGO algorithm may not cross-validate properly if there are trends in the data, in contrast to NEGO which is expected to subtract any significant trends in the data.

The benefits of modeling deterministic functions using this probabilistic approach are: i) represents a best linear unbiased estimator, ii) interpolates the data, and iii) provides error estimates.

Figure of merit. With reference to **Fig 1**, there are two zones where it is desirable to add additional points. The zone (left) where the objective function is minimized and the zone (right) where there is a significant error in the prediction. Hence the figure of merit for adding sample points should be high in either of these situations. Specifically, the figure of merit[6] used in this work, is given by Eq. 6.

$$fom(x) = \left(f_{min} - \hat{y}\right)\Phi\left(\frac{f_{min} - \hat{y}}{s}\right) + s\phi\left(\frac{f_{min} - \hat{y}}{s}\right) \quad (6)$$

where Φ and ϕ are the cumulative and density normal distribution functions, respectively; and $f_{\min}$ denotes the minimum current objective function value. Eq. 6 establishes the desired balance of sampling where the response surface (the predictor) is minimized (left term) and in zones where error estimates are high (right term). Note that the figure of merit makes reference to the objective function so it includes the sum of the output of both the neural network and the residual models.

This surface response approach for global optimization is expected to outperform competing methods, in terms of necessary computationally expensive objective function evaluations, to meet an stopping criteria. It can identify promising areas without the need of moving step by step along a given trajectory. In addition, by providing estimates of the errors at unsampled points, it is possible to establish a reasonable stopping criterion. Furthermore, provides a fast surrogate model that could be used to visualize the relationship between the sought parameters and the objective function values and to identify the relative significance of each of the parameters.

Implementation. The following case studies were solved using an implementation of the NEGO algorithm developed by the authors in Matlab[8] Ver. 5.3. The subproblems of finding near optimal values for maximizing likelihood and the figure of merit were solved using the DIRECT method[9]. Note that the solution of these subproblems do not require additional computationally expensive objective function evaluations. The reservoir numerical simulations were conducted using a commercial reservoir numerical simulator (EXODUS Ver. 4.1[10]).

Case studies

The NEGO algorithm was evaluated using two case studies of increasing complexity (from 6 to 23 independent parameters). The case studies consider reservoirs similar to those found in well-known benchmark cases[11,12]. In both instances, the dynamic and static data were obtained assuming the permeability and porosity parameters were known (later called "correct" values). Then, the problems were posed in inverse fashion; that is, given dynamic and static data associated with a reservoir; what are the parameter values that reproduce the available dynamic and static data?.

The first case study addresses the integration of dynamic data (cumulative oil production and gas-oil ratio), while the second case considers the integration of both dynamic (cumulative oil production and gas-oil ratio) and static data (a variogram model). In both cases, the production data is available yearly, for a period of ten (10) years, and in the second case study the covariance is calculated using ten (10) intervals.

Case study No. 1. The reservoir under consideration and the coordinate system used, are illustrated in **Fig. 2**. It is assumed that production data (i.e. COP and GOR) are available and that certain permeability and porosity parameters are unknown.

With reference to **Fig. 3**, the reservoir is at a depth of 8325 ft., has an initial pressure of 4800 psi., and initial oil and water saturations of 0.8, and 0.2, respectively. The numerical grid is composed of 10x10x3 blocks in the x, y and z directions. The injector and producer wells are placed in the blocks denoted as (10,10,3) and (1,1,1), respectively. The porosity is assumed to be constant throughout the reservoir, the horizontal permeability is isotropic, but, as the vertical permeability, is different for each of the layers.

In this case, the unknown parameters and the restrictions on their possible values are presented in Table 1, and the objective function is given by Eq. 7.

$$f(x)=\sum_{i=1}^{10}\left[\frac{COP_{obs_i}-COP_{calc_i}}{COP_{obs_i}}\right]^2+\sum_{i=1}^{10}\left[\frac{GOR_{obs_i}-GOR_{calc_i}}{GOR_{obs_i}}\right]^2 \quad ....(7)$$

The neural network and DACE models were constructed using a sample of sixty (60) points selected using a latin hypercube sampling procedure. Twenty (20) additional points were added in the search of the "correct" permeability and porosity parameters.

Case study No. 2. The reservoir under consideration and the coordinate system used, are illustrated in **Fig. 4**. It is assumed that dynamic data (i.e. COP and CGOR) and static data (variogram model) are available and that certain permeability and porosity parameters are unknown.

With reference to **Fig. 5**, the reservoir is at a depth of 8375 ft., has an initial pressure of 4800 psi., and initial oil and gas saturations of 1.0, and 0.0, respectively. The numerical grid is composed of 10x10x4 blocks in the x, y and z directions. The producer wells 1 and 2, are placed in the blocks denoted by (10,1,1), and (1,10,1) respectively. The injector well is placed in the block (1,1,1). The porosity varies among layers with 0.30 for layer 1, 0.20 for layer 2, and 3, and 0.10 for layer 4. The numerical grid was grouped into twenty (20) zones, distributed among the different layers as depicted in **Figs. 6-9**. The permeability is considered to be the same within a given zone and does not change with coordinate direction (isotropic).

In this case, the unknown parameters and the restrictions on their possible values are presented in Table 2, and the objective function is given by Eq. 8.

$$f(x)=\sum_{i=1}^{10}\left[\frac{COP_{obs_i}-COP_{calc_i}}{COP_{obs_i}}\right]^2+\sum_{i=1}^{10}\left[\frac{CGOR_{obs_i}-CGOR_{calc_i}}{CGOR_{obs_i}}\right]^2+$$
$$+\sum_{i=1}^{10}\left[\frac{COV_{obs_i}-COV_{calj_i}}{COV_{obs_i}}\right]^2 \quad ....(8)$$

The neural network and DACE models were constructed using a sample of one hundred and eighty six (187) points selected using a latin hypercube sampling procedure. Eighty (80) additional points were added in the search of the "correct" permeability and porosity parameters.

Results and discussion

With reference to **Case study No. 1**, the neural network was constructed with an 6x2x1 architecture with a sum of square errors of 5.82e-002, and 9.68e-002, respectively. Additionally, all the points in the DACE model cross-validated within three times of the standard deviation. The minimum objective function value found within the initial sample (60 points) was 2.17e-03. Additional points (20) were added so that the figure of merit was maximized; from those points the best solution found (8th additional sampled point) observed an objective function value of 3.46e-04, that is an order of magnitude lower than the best found in the initial sample. The parameter values and the objective function value for the additional points are shown in Table 3. The maximum percentage error in the parameters estimation (K1, K2, K3, K4, K5, P) is 10%, as illustrated in **Fig. 10**. The maximum percentage errors in the estimation of COP and GOR, were 0.18%, and 0.45%, respectively. **Figs. 11 and 12** shows the excellent agreement between the values of COP and GOR obtained using the "correct" parameters and those found by the NEGO algorithm. Note that the results were obtained using only 80 computationally expensive objective function evaluations.

With reference to **Case study No. 2**, the neural network was constructed with a 23x3x1 architecture with a sum of square errors of 4.97e-002 and 9.05e-002, respectively. A 98% of the points in the DACE model cross-validated within three times of the standard deviation. The minimum objective function value found within the initial sample (187 points) was 2.16e-02. Additional points (80) were added so that the figure of merit was maximized; from those points the best solution found (56th additional sampled point) observed an objective function value of 1.37e-02, that is approximately 50% lower than the best found in the initial sample. The parameter values and the objective function value for the additional points are shown in Table 4. The maximum percentage error in the parameters estimation is approximately 20%, as illustrated in **Fig. 13**. The maximum percentage errors in the estimation of COP and CGOR, and COV were 0.79%, 6.81%, and 8.09%, respectively. **Figs. 14 and 15** shows the excellent agreement between the values of COP and CGOR obtained using the correct parameters and those found by the proposed solution methodology. **Fig. 16** depicts the agreement between the desired variogram and that obtained using the NEGO algorithm. Note that the results were obtained using only 267 computationally expensive objective function evaluations.

From the results it is concluded that the methodology can be used effectively and efficiently for reservoir characterization purposes. In addition, the optimization approach holds promise to be useful in the optimization of objective functions involving the execution of computationally expensive mathematical models (e.g. reservoir numerical simulators), such as those found, not only in reservoir characterization, but also in other areas of petroleum engineering (e.g. EOR optimization).

Conclusions

- A global optimization method for integrating static and dynamic data into a reservoir description, called NEGO has been proposed. The method includes the construction of a "fast surrogate" of an objective function whose evaluation involves the execution of a time-consuming mathematical model (i.e. reservoir numerical simulator) based on neural networks, DACE modeling, and adaptive sampling. Using adaptive sampling, promising areas are searched considering the information provided by the surrogate model and the expected value of the errors.

- The results suggest that the NEGO algorithm can be used effectively and efficiently for reservoir characterization purposes. In addition, the optimization approach holds promise to be useful in the optimization of objective functions involving the execution of computationally expensive mathematical models (e.g. reservoir numerical simulators), such as those found, not only in reservoir characterization, but also in other areas of petroleum engineering (e.g. EOR optimization).
- The NEGO algorithm is expected to outperform competing methods, in terms of computationally expensive objective function evaluations, necessary to meet an stopping criteria. This is because it can identify promising areas without the need of moving step by step along a given trajectory. In addition, by providing estimates of the errors at unsampled points, it is possible to establish a reasonable stopping criteria. Furthermore, provides a fast surrogate model that could be used to visualize the relationship between the sought parameters and the objective function values and to identify the relative significance of each of the parameters.

Nomenclature

DACE = Design and analysis of computer experiment
x = Parameters vector
X = Set constraint
f = Objective function
W = Weighting matrix
d_{obs} = Reference to static and dynamic data available (normalized)
d_{cal} = Denotes the data obtained using a mathematical model
y = DACE response value
μ = Mean of the population
ε = Error in the DACE model
p = Number of dimensions in the vector x
σ = Standard deviation of the population
θ_h = Correlation parameter
r' = Correlation vector between the new point and the points used to construct the model
R = Correlation matrix between the n sample points
1 = n-vector of ones
fom = Figure of merit
Φ = Cumulative normal distribution function
ϕ = Density normal distribution function
$\hat{y}$ = DACE predictor
fmin = Current best function value
$s^2(x)$ = Mean square error of the predictor
COP = Cumulative oil production
CGOR = Cumulative gas oil ratio
GOR = Gas oil ratio
COV = Covariance
. BIS = Best initial solution

Subscripts
h = Coordinate directions
obv = Observed
cal = Calculated

Superscript
* = New point
' = Transpose

Acknowledgments

The authors gratefully acknowledge the financial support provided by the Consejo Nacional de Investigaciones Petroleras (CONIPET) and the Consejo Nacional de Investigaciones Científicas (CONICIT), Venezuela, to execute this project.

References

1. Sacks, J., Welch, W., Mitchell, T., and Wynn, H., "Design and Analysis of Computer Experiments", *Statistical Science*, Vol. 4, pp. 409-435.
2. Tan, T., "A Computationally Efficient Gauss-Newton Method for Automatic History Matching", paper SPE 29100 presented at the SPE 13th Symposium on Reservoir Simulation held in San Antonio, Texas, February, 12-15.
3. Landa, J., and Horne, R., "A Procedure to Integrate Well Test Data, Reservoir Performace History and 4-D Seismic Information into a Reservoir Description", paper SPE 38653 presented at the 1997 SPE Annual Technical Conference and Exhibition held in San Antonio, Texas, October 5-8.
4. Huang, X., Kelkar, M., "Application of Combinatorial Algorithms for Description of Reservoir Properties", paper SPE/DOE 27803 presented at the 1994 Ninth Symposium on Improved Oil Recovery, Tulsa, Oklahoma, April 17-20.
5. M.K. Akhll Dtta Gupta, P.L. Stoffa, L.W. Lake, and G.A. Pope, U. Of Texas, "Stochastic Reservoir Modeling Using Simulated Annealing and Genetic Algorithm", paper SPE 24754 presented at the 1992 67 th SPE Annual Technical Conference and Exhibition held in San Antonio, Texas, October 4-7.
6. Jones, D., Schonlau, M., and Welch, W., "Efficient Global Optimization of Expensive Black-Box Functions", *Journal of Global Optimization*, Vol. 13, 1998, pp. 455-492.
7. McKay, M., Beckman, R., and Conover, W., "A Comparison of Three Methods for Selecting Values of Input Variables in the Analysis of Output from a Computer Code", *Technometrics*, Vol. 21, No. 2, May, 1979, pp. 239-245.
8. MATLAB, Ver. 5.3. The MathWorks Inc.

9. Jones, D., Perttunen, C., and Stuckman, B., "Lipschitzian Optimization Without the Lipschitz Constant", Journal of Optimization Theory and Applications, Vol. 79, No. 1, October 1993, pp. 157-181.
10. EXODUS, Ver. 4.1. T.T & Associates Inc.
11. Aziz, S. Odeh, "Comparison of Solutions to a Three-Dimensional Black-Oil Reservoir Simulation Problem", paper SPE 9723, January, 1981.
12. Quandalle, P. "Eight SPE Comparative Solution Project: Gridding Techniques in Reservoir Simulation", paper SPE 25263 presented at the 1993 12th SPE Symposium on Reservoir Simulation, New Orleans, LA, U.S.A, February 28 – March 3.

TABLE 1 - PERMEABILITY AND POROSITY PARAMETERS (CASE STUDY No. 1)

Variable	Description	Range		Units
K1	Permeability in the x and y directions. Layer 1	450	650	md
K2	Permeability in the x and y directions. Layer 2	35	55	md
K3	Permeability in the x and y directions. Layer 3	160	240	md
K4	Permeability in the z direction. Layer 1	52	82	md
K5	Permeability in the z direction. Layers 2 and 3	22	32	md
P	Porosity. Layers 1, 2 and 3	0.25	0.37	-

TABLE 2- PERMEABILITY AND POROSITY PARAMETERS (CASE STUDY No. 2)

Variable	Description	Range		Units
K11	Permeability zone 1, Layer 1	432	624	md
K12	Permeability zone 2, Layer 1	345	525	md
K13	Permeability zone 3, Layer 1	400	600	md
K14	Permeability zone 4, Layer 1	340	480	md
K15	Permeability zone 5, Layer 1	376	540.5	md
K21	Permeability zone 1, Layer 2	43.2	62.4	md
K22	Permeability zone 2, Layer 2	31.5	49.5	md
K23	Permeability zone 3, Layer 2	40	60	md
K24	Permeability zone 4, Layer 2	34	48	md
K25	Permeability zone 5, Layer 2	37.6	54.05	md
K31	Permeability zone 1, Layer 3	16.2	23.4	md
K32	Permeability zone 2, Layer 3	11.2	17.6	md
K33	Permeability zone 3, Layer 3	16	24	md
K34	Permeability zone 4, Layer 3	12.75	18	md
K35	Permeability zone 5, Layer 3	13.6	19.55	md
K41	Permeability zone 1, Layer 4	8.1	11.7	md
K42	Permeability zone 2, Layer 4	4.9	7.7	md
K43	Permeability zone 3, Layer 4	8	12	md
K44	Permeability zone 4, Layer 4	4.25	6	md
K45	Permeability zone 5, Layer 4	6.4	9.2	md
P1	Porosity. Layer 1	0.27	0.39	-
P2,3	Porosity. Layers 2 and 3	0.14	0.22	-
P4	Porosity. Layer 4	0.08	0.12	-

TABLE 3 – ADDITIONAL SAMPLED POINTS (CASE STUDY NO. 1)

Obs.	K1	K2	K3	K4	K5	P	*f.*
1	483.33	51.67	200	67	30.33	0.31	0.00037604
2	550	38.33	226.67	57	23.67	0.31	0.00373747
3	616.67	45	173.33	67	27	0.31	0.0420268
4	483.33	38.33	226.67	67	27	0.35	0.08506395
5	616.67	51.67	200	57	27	0.35	0.02255316
6	483.33	38.33	226.67	67	27	0.31	0.02850679
7	550	51.67	200	57	23.67	0.31	0.04083019
8	483.33	45	200	77	23.67	0.31	0.00034579
9	550	38.33	173.33	57	27	0.35	0.00852373
10	550	38.33	226.67	77	30.33	0.31	0.01906443
11	616.67	38.33	200	67	27	0.35	0.01527427
12	483.33	51.67	226.67	67	27	0.31	0.06371478
13	483.33	38.33	200	57	30.33	0.31	0.00348125
14	550	38.33	200	57	30.33	0.35	0.05410506
15	550	38.33	173.33	67	23.67	0.35	0.00800637
16	483.33	45	226.67	57	30.33	0.31	0.03427427
17	483.33	45	173.33	67	30.33	0.31	0.07724744
18	550	51.67	226.67	67	30.33	0.31	0.00908735
19	616.67	45	200	57	23.67	0.35	0.01946102
20	550	45	200	57	23.67	0.35	0.06582813

TABLE 4 - NEGO ESTIMATES FOR THE PERMEABILITY AND ´POROSITY PARAMETERS (CASE STUDY No. 2)

Variable	"Correct" Value	BIS	Error (%)	Best Solution	Error (%)
K11	480	474.47	1.152	592	23.333
K12	450	402.384	10.581	435	3.3333
K13	500	472	5.6	500	0
K14	400	361.882	9.529	363.333	9.166
K15	470	495.345	5.392	403.417	14.1667
K21	48	46.577	2.964	46.4	3.3333
K22	45	42.730	5.044	40.5	10
K23	50	45.972	8.056	50	0
K24	40	46.412	16.031	41	2.5
K25	47	49.709	5.764	45.825	2.5
K31	18	20.038	11.32	19.8	10
K32	16	12.418	22.384	14.4	10
K33	20	23.607	18.036	20	0
K34	15	17.219	14.799	15.375	2.5
K35	17	15.959	6.122	16.575	2.5
K41	9	8.455	6.06	9.9	10
K42	7	6.905	1.348	6.3	10
K43	10	10.416	4.168	10	0
K44	5	5.831	16.619	5.125	2.5
K45	8	6.935	13.311	7.8	2.5
P1	0.3	0.304	1.472	0.33	10
P2,3	0.2	0.1904	4.78	0.18	10
P4	0.1	0.0815	18.408	0.1	0
	f	**0.0216**	**-**	**0.0137**	**-**

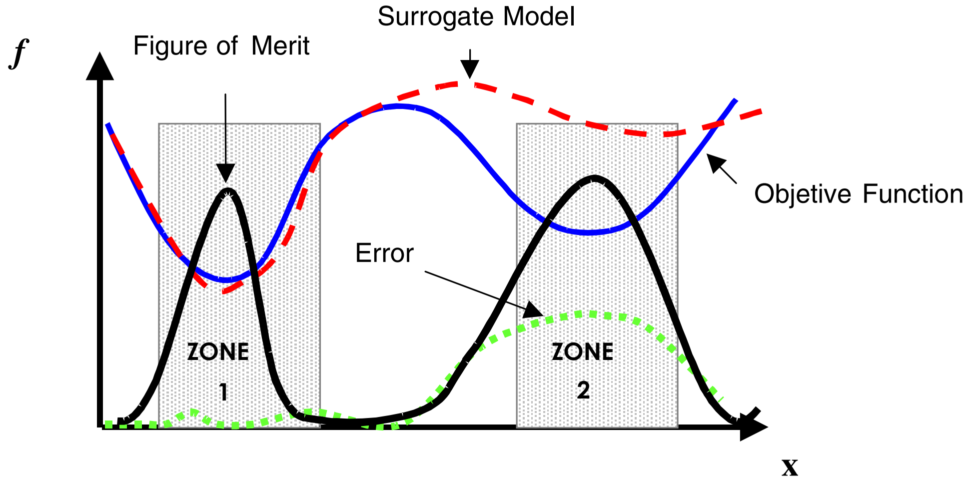

Fig. 1.- Illustration of the purpose of the figure of merit

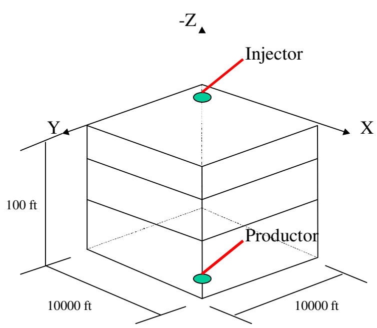

Fig. 2.-Reservoir illustration (Case Study No. 1)

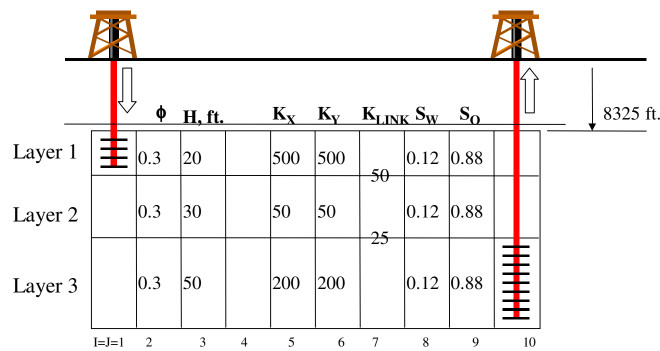

Fig. 3.-Schematic representation of the reservoir considered in (Case Study No. 1)

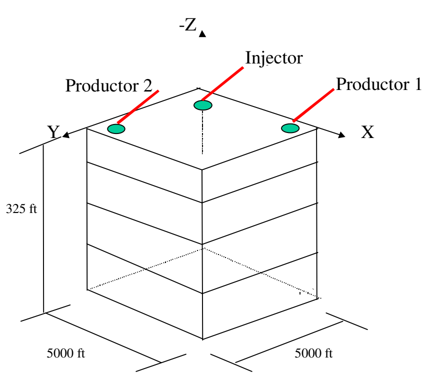

Fig. 4.-Reservoir illustration (Case Study No. 2)

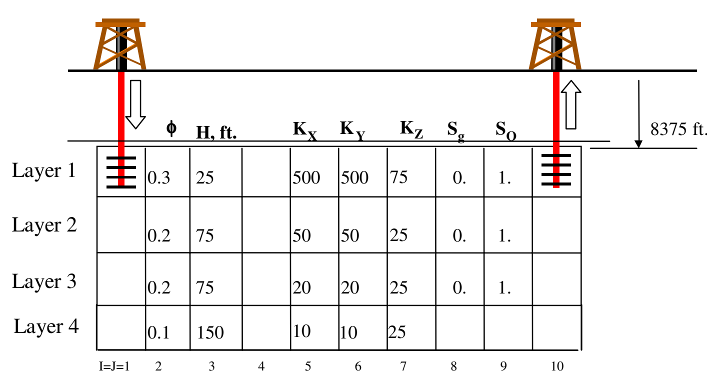

Fig. 5.-Schematic representation of the reservoir considered in (Case Study No. 2)

	1	2	3	4	5	6	7	8	9	10
1	1.	1.	1.	1.	1.	1.	1.	3.	3.	3.
2	1.	1.	1.	1.	1.	1.	1.	3.	3.	3.
3	1.	1.	1.	1.	2.	2.	2.	3.	3.	3.
4	1.	1.	1.	1.	2.	2.	2.	2.	4.	4.
5	1.	1.	1.	1.	2.	2.	2.	2.	4.	4.
6	3.	3.	3.	2.	2.	2.	2.	2.	4.	4.
7	3.	3.	3.	2.	2.	2.	2.	2.	4.	4.
8	3.	3.	3.	5.	5.	5.	5.	4.	4.	4.
9	3.	3.	3.	5.	5.	5.	5.	4.	4.	4.
10	3.	3.	3.	5.	5.	5.	5.	4.	4.	4.

Fig. 6.- Zones 1 – 5 in layer1.(Case study No. 2)

	1	2	3	4	5	6	7	8	9	10
1	6.	6.	6.	6.	6.	6.	6.	8.	8.	8.
2	6.	6.	6.	6.	6.	6.	6.	8.	8.	8.
3	6.	6.	6.	6.	7.	7.	7.	8.	8.	8.
4	6.	6.	6.	6.	7.	7.	7.	7.	9.	9.
5	6.	6.	6.	6.	7.	7.	7.	7.	9.	9.
6	8.	8.	8.	7.	7.	7.	7.	7.	9.	9.
7	8.	8.	8.	7.	7.	7.	7.	7.	9.	9.
8	8.	8.	8.	10.	10.	10.	10.	9.	9.	9.
9	8.	8.	8.	10.	10.	10.	10.	9.	9.	9.
10	8.	8.	8.	10.	10.	10.	10.	9.	9.	9.

Fig. 7.- Zones 6 – 10 in layer 2.(Case study No. 2)

	1	2	3	4	5	6	7	8	9	10
1	11.	11.	11.	11.	11.	11.	11.	13.	13.	13.
2	11.	11.	11.	11.	11.	11.	11.	13.	13.	13.
3	11.	11.	11.	11.	12.	12.	12.	13.	13.	13.
4	11.	11.	11.	11.	12.	12.	12.	12.	14.	14.
5	11.	11.	11.	11.	12.	12.	12.	12.	14.	14.
6	13.	13.	13.	12.	12.	12.	12.	12.	14.	14.
7	13.	13.	13.	12.	12.	12.	12.	12.	14.	14.
8	13.	13.	13.	15.	15.	15.	15.	14.	14.	14.
9	13.	13.	13.	15.	15.	15.	15.	14.	14.	14.
10	13.	13.	13.	15.	15.	15.	15.	14.	14.	14.

Fig. 8.- Zones 11 – 15 in layer 3. (Case study No. 2)

	1	2	3	4	5	6	7	8	9	10
1	16.	16.	16.	16.	16.	16.	16.	18.	18.	18.
2	16.	16.	16.	16.	16.	16.	16.	18.	18.	18.
3	16.	16.	16.	16.	17.	17.	17.	18.	18.	18.
4	16.	16.	16.	16.	17.	17.	17.	17.	19.	19.
5	16.	16.	16.	16.	17.	17.	17.	17.	19.	19.
6	18.	18.	18.	17.	17.	17.	17.	17.	19.	19.
7	18.	18.	18.	17.	17.	17.	17.	17.	19.	19.
8	18.	18.	18.	20.	20.	20.	20.	19.	19.	19.
9	18.	18.	18.	20.	20.	20.	20.	19.	19.	19.
10	18.	18.	18.	20.	20.	20.	20.	19.	19.	19.

Fig. 9.-. Zones 16 – 20 in layer 4. (Case study No. 2)

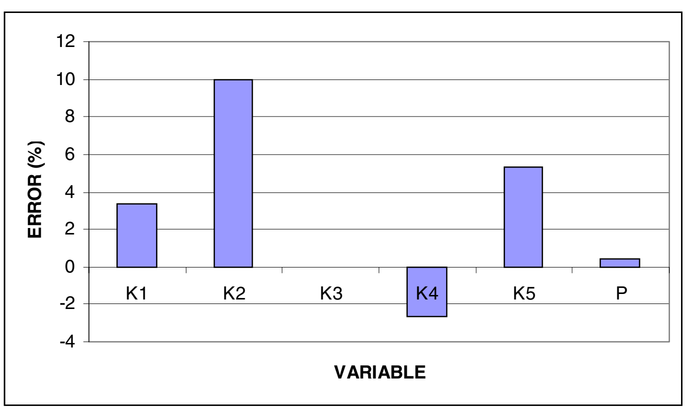

Fig. 10.- Distribution of the error in parameter estimations. (Case Study No. 1)

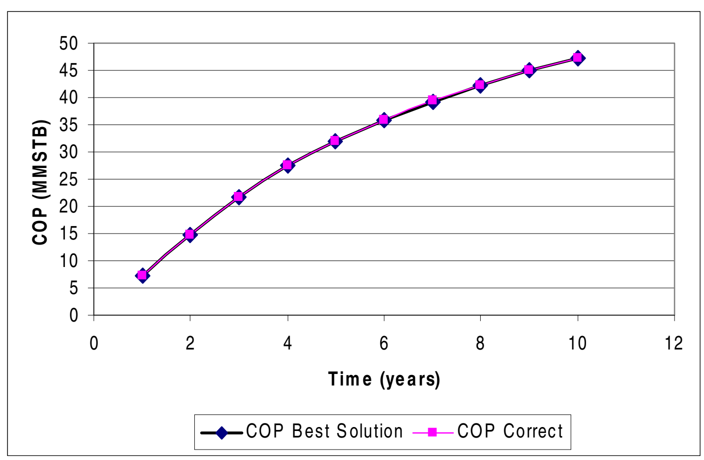

Fig. 11.-Cumulative oil production obtained using the best solution and the "correct" solution (Case Study No. 1)

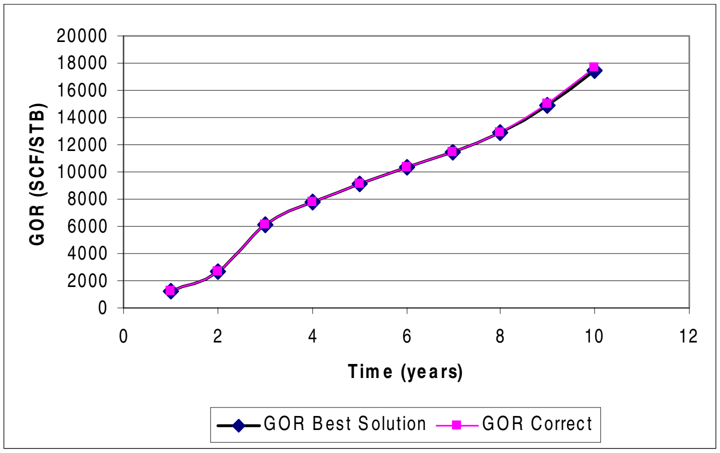

Fig. 12.-Gas oil ratio obtained using the best solution and the "correct" solution (Case Study No. 1)

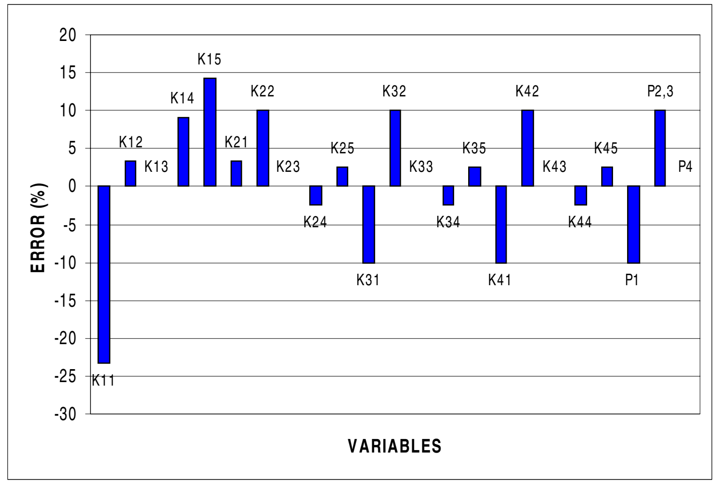

Fig. 13.-Distribution of the error in parameter estimations. (Case Study No. 2)

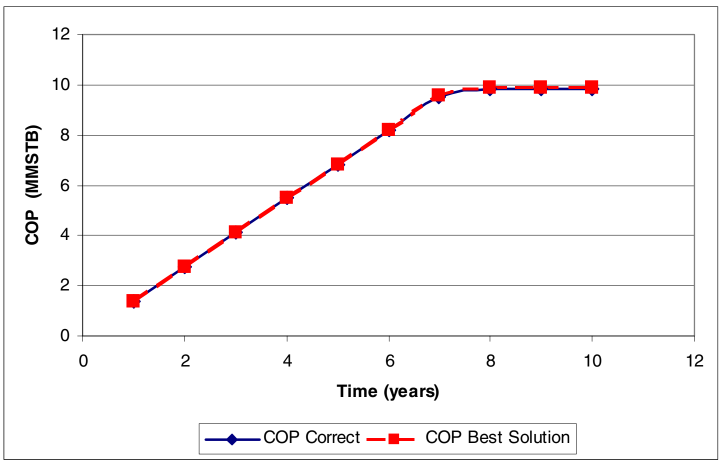

Fig. 14.-Cumulative oil production obtained using the best solution and the "correct" solution (Case Study No. 2)

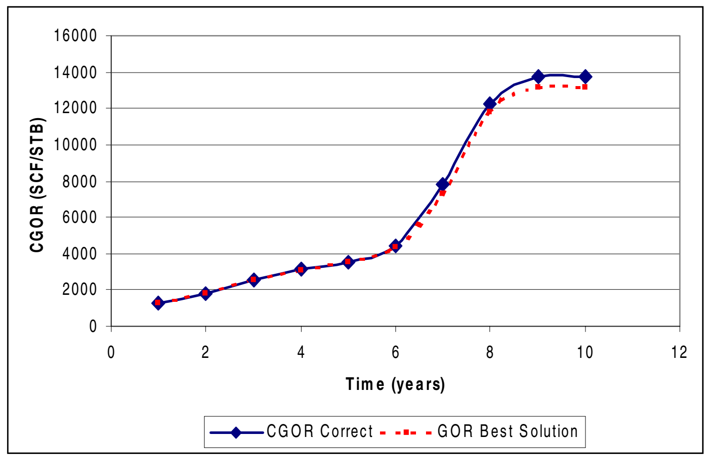

Fig. 15.-Cumulative gas oil ratio obtained using the best solution and the "correct" solution (Case Study No. 2)

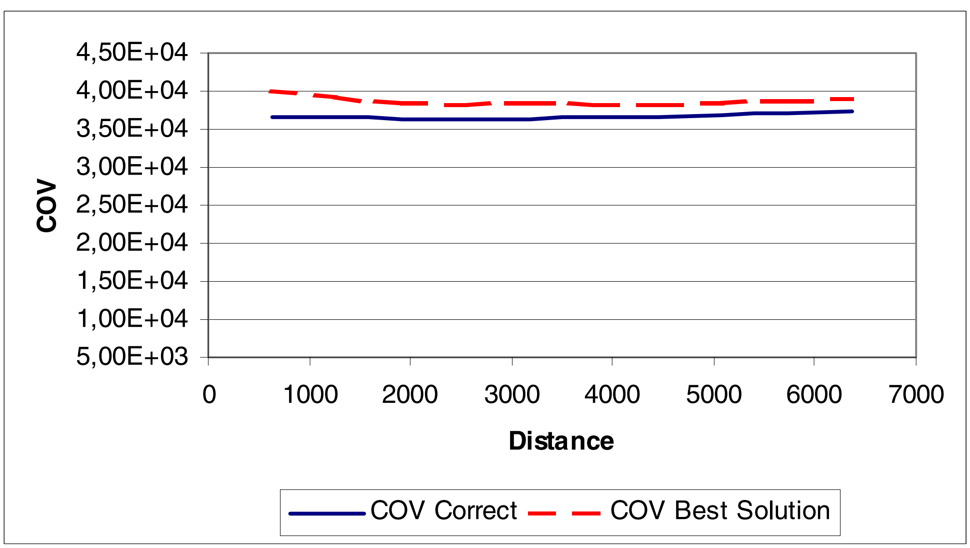

Fig. 16.-Covariance values obtained using the best solution and "correct" value of horizontal permeability parameter